Nanoscale

Accepted Manuscript

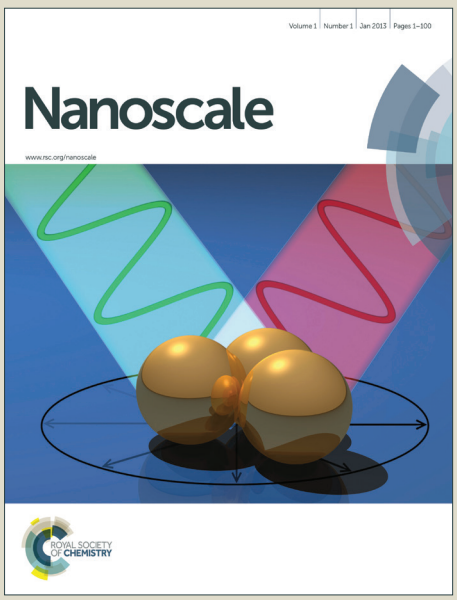

This is an *Accepted Manuscript*, which has been through the Royal Society of Chemistry peer review process and has been accepted for publication.

Accepted Manuscripts are published online shortly after acceptance, before technical editing, formatting and proof reading. Using this free service, authors can make their results available to the community, in citable form, before we publish the edited article. We will replace this *Accepted Manuscript* with the edited and formatted *Advance Article* as soon as it is available.

You can find more information about *Accepted Manuscripts* in the Information for Authors.

Please note that technical editing may introduce minor changes to the text and/or graphics, which may alter content. The journal's standard Terms & Conditions and the Ethical guidelines still apply. In no event shall the Royal Society of Chemistry be held responsible for any errors or omissions in this *Accepted Manuscript* or any consequences arising from the use of any information it contains.

ROYAL SOCIETY OF CHEMISTRY

www.rsc.org/nanoscale

Cite this: DOI: 10.1039/c0xx00000x

www.rsc.org/xxxxxx

ARTICLE TYPE

Amphiphilic Copolymer Coated Upconversion Nanoparticles for Near-Infrared Light-Triggered Dual Anticancer Treatment

Shun Yang [a], Najun Li* [a], Zhuang Liu [b],Wenwei Sha [a], Dongyun Chen [a], Qingfeng Xu [a] and Jianmei Lu* [a]

Received (in XXX, XXX) Xth XXXXXXXXX 20XX, Accepted Xth XXXXXXXXX 20XX

DOI: 10.1039/b000000x

The light-triggered controlled release of anticancer drugs accompanied with NIR-responsive photodynamic therapy was prepared *via* self-assembly. Firstly, Mn^{2+}-doped upconversion nanoparticles (UCNPs) were coated with mesoporous silica shell and modified with photosensitizer (Chlorin e6) and long alky chains. And then the NIR light-responsive amphiphilic copolymer containing 9,10-dialkoxyanthracene groups was synthesized and then coated as the outermost layer. Upon the irradiation of 980 nm laser, the CCUCNPs@PM would absorb and then convert the NIR light to higher-energy visible red light (660 nm) by the UCNPs-based core, which could excite Chlorin e6 (Ce-6) to produce singlet oxygen ($^1O_2$). Then the $^1O_2$-sensitive dialkoxyanthracene group in the amphiphilic copolymer would be degraded and detached from the surface of the CCUCNPs@PM, following with the controlled release of the pre-loaded drugs and the photodynamic therapy for cancer cells caused by the excess $^1O_2$. In vitro and in vivo experiments also demonstrated that the drug-loaded CCUCNPs@PM possessed better therapeutic efficacy compared with vacant one. Therefore, the NIR light-controlled chemotherapy and photodynamic therapy could be realized simultaneously by CCUCNPs@PM.

Introduction

Controlled drug release systems that respond to environmental stimulus were always used to conquer the drawback of chemotherapy such as systemic toxicity, low therapeutic efficacy and other side effects in cancer treatment.[1-4] As promising tools for controlled drug release, photo trigger-controlled drug-release devices (PDDs) have attracted much attention owing to their on-demand release and improved therapeutic efficacy.[5] To date, a handful of PDDs based on the scaffolds such as azobenzene, o-nitrobenzyl and spiropyran have been developed, and the bioactive specie release is typically trigged by photolysis with ultraviolet/visible light. [6-10] However, the high-energy light (~6 eV) can hardly penetrate the tissue and is harmful to normal physiological organizations, which hampers its potential use in further in vivo biomedical applications.[11,12]

Recently, some photo-responsive inorganic nanoparticles were introduced to overcome these drawbacks so that continuous-wave NIR light could be used to trigger the drug release. For instance, gold nanoparticles/rods were coated with temperature-responsive polymer/DNA for photo-triggered drug release via a photothermal conversion process.[13,14] Upconversion nanoparticles (UCNPs), which can absorb NIR light and convert to higher-energy photons in the UV/visible regions, were introduced into the typical PDDs to control the release process *in vivo* by NIR light.[15-17] Although remarkable achievements have been attained in the field of NIR light trigger-controlled drug-release devices, exploring various novel stimuli-responsive systems is always an important goal for the development of PDDs.

Besides, Photodynamic therapy (PDT) attracts more and more interests in the cancer treatment recently.[18,19] Photosensitizer (PS) molecules can produce cytotoxic reactive oxygen species (ROS) and singlet oxygen ($^1O_2$) to kill nearby cancer cells upon appropriate irradiation of light.[20] Current PDT uses visible or even UV light to excite photosensitizers, and thus suffers from the rather limited light-penetration in biological tissues.[21] To conquer this problem, several groups have been attracted by inorganic UCNPs. Under NIR light excitation, UCNPs are able to emit visible light, which can activate surrounding PS molecules to produce singlet oxygen to kill cancer cells. In order to improve the PDT to selectively treat the lesion region, stimuli-responsive $^1O_2$ release may be favorable.[22-25]

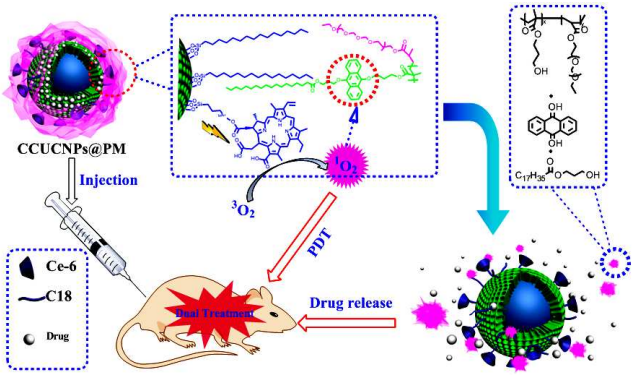

Scheme 1 Schematic illustration of the NIR light trigger-controlled drug-release and NIR-responsive photodynamic therapy of nanocomposites.

In this work, a new core-shell nanocomposite was fabricated for controlled release of anticancer drugs accompanied with PDT

Nanoscale Accepted Manuscript

treatment both triggered by NIR light. As shown in Scheme 1, Mn^{2+}-doped UCNP was first coated with mesoporous silica and then modified with long alky chain and Chlorin e6 (Ce-6). The modified nanoparticles (CCUCNPs) were then encapsulated with a $^1O_2$-responsive amphiphilic copolymer *via* a simple self-assembly process. Upon NIR light (980 nm) irradiation, UCNPs would absorb NIR light and convert it to higher-energy visible red light (660 nm) which could excite Ce-6 to produce singlet oxygen ($^1O_2$). The 9,10-dialkoxyanthracene (DN) groups in the amphiphilic copolymer would be changed into 9,10-anthraquinone (AQ) by $^1O_2$ excitation, followed by the degradation of the polymer. After detached from the surface of CCUCNPs, the loaded drug would release from the nanocomposite and excess $^1O_2$ also was able to kill tumour cells. Furthermore, the as-prepared Mn^{2+}-doped UCNP with strong red upconversion (UC) emission are able to provide a second imaging capacity as magnetic resonance (MR) imaging probes and could be used as potential bio-labels for *in vivo* imaging. As a result, the prepared nanocomposite could be potentially employed for both controlled drug release of anticancer drugs and photodynamic therapy triggered by NIR light as well as in vivo bioimaging.

Experimental Section

Materials: All chemicals, unless specified otherwise, were purchased from Sigma-Aldrich and used as received. All cell-culture related reagents were purchased from Hyclone.

Instrumentation: The FT-IR measurements were performed as KBr pellets on aNicolet 4700 spectrometer (Thermo Fisher Scientific) in therange 400–4000 cm^{-1}. The ^{1}HNMR spectra were measured on an INOVA 400 MHz NMR instrument.TEM images were taken by a TecnaiG220 electron microscope operating at 200 kV. The number average molecular weight (M_n) using a Waters 1515 pump.The Brunauer–Emmett–Teller (BET) and Barrett–Joyner–Halenda (BJH) analyses were used to determine the surface area, pore size and pore volumeand were obtained with a Quanta chromeAutosorb 1C apparatus at -196 ^{o}C under continuous adsorption conditions. Powder X-ray diffraction wasrecorded on PAN alytical XRD diffractometer using Cu-Ka radiation. The UV-Vis absorption spectra were recorded by a Perkin-Elmer Lambda-17 Spectrophotometer. Fluorescent emission spectra were measured by a FluoroMax-4 luminescent spectrometer (HORIBA JobinYvon S.A.S) using a 980 nm laser diode as the excitation source.

CCUCNPs: Mn^{2+} ion-doped $NaY(Mn)F_4$:Yb/Er nanocrystals (Y:Mn:Yb:Er = 50:30:18:2) were prepared as reported previously.[28] To improve the hydrophilic nature of UCNPs, a typical procedure was followed: the as-synthesized nanoparticles (7.5 mg) were centrifuged and transferred to chloroform solutions. The chloroform solutions (1 mL) were then redispersed in 10 mL CTAB solutions (0.1 M) and sonicated for more than 2 h until the chloroform evaporated. The resulting nanoparticles were collected using centrifugation and then washed three times with distilled water.

The mesoporous silica-coated UCNPs ($UCNPs@mSiO_2$) were synthesized as follows: 0.5 mL of UCNPs@CTAB solution was dispersed in 10 mL of CTAB (5.4 mM) and NaOH solution (1.4 mM). Next, 0.075 mL of TEOS was added dropwise into the mixture solution and stirred vigorously at 55 ^{o}C in a wate bath for 4 h. While the $UCNPs@mSiO_2$ nanoparticles were being prepared, some aggregates yielding white precipitates were observed. To completely remove these aggregates, the $UCNPs@mSiO_2$ colloidal solutions were centrifuged at 3500 rpm for 5 min, and the supernatants were collected for further preparation. Subsequently, C18/ethanol extraction was used to remove the CTAB from the mesoporous silica shells of $UCNPs@mSiO_2$ nanoparticles

The 5 mg of $UCNPs@mSiO_2$ nanoparticles were then suspended in ethanol at 80 ^{o}C using a reflux process. C18 (0.5 mL) was added to yield $UCNPs@mSiO_2@C18$ nanoparticles. $UCNPs@mSiO_2@C18$ colloidal solutions were centrifuged at 15000 rpm for 15 min to remove excess CTAB surfactants. The collected precipitates ($UCNPs@mSiO_2@C18$ nanoparticles) were washed in ethanol for three times.

25 mg Ce-6 was activated by 8 mg EDC (1.0 eq) and 5 mg NHS (1.0 eq) in 5 mL anhydrous DMSO for 30 min. The activated Ce-6-NHS was then added into 10 mg APTES dissolved in ethanol. After 24 h of reaction, 10 mg $UCNPs@mSiO_2@C18$ nanoparticles were added and the mixture was stirred for another 24 h. The resulting products were collected using centrifugation and then washed with ethanol several times, and dried under vacuum to get $UCNPs@mSiO_2@C18@Ce-6$ (CCUCNPs).

Synthesis of PEG-b-MAPS (PM): hydrophobic monomer 3-((10-(3-(methacryloyloxy)propoxy) anthracen-9-yl)oxy) propylstearate (MAPS) was synthesized as previously reported.

The amphiphilic diblock polymer PM was synthesized by Free Radical polymerization. In a typical procedure, 1.2 g of Poly(ethylene glycol) methyl ether methacrylate-950 was added to a dimethylsulfoxide solution containing 3 mg AIBN and 200 mg (0.31 mmol) MAPS and then placed in an oil bath at 70 ^{o}C for 5 h. The mixture was concentrated and washed with a large amount of ethyl ether. After washing, the obtained diblock polymer was dried under vacuum overnight and stored in desiccators.

Preparation of CCUCNPs@PM: PM (PEG-b-MAPS) (20 mg) was dissolved into 1 mL tetrahydrofuran, and then CCUCNPs (10 mg) dispersed in this mixture by sonication for 5 min. Then, 5 mL of distilled water was added to the above mixture with vigorous shaking and the resulting colloid was stirred continues vigorously for 24 h at room temperature to evaporate tetrahydrofuran. The prepared nanoparticles were achieved by centrifugation and washed by water, dried under vacuum overnight and stored in desiccators for further use.

Drug Loading: Doxorubicin (DOX) was used as a model anticancer agent. Free water-insoluble DOX was extracted from doxorubicin hydrochloride (DOX·HCl) according to the procedure reported previously. The DOX solution (5 mg mL^{-1}) was added in the procedure of preparation CCUCNPs@PM. Then, the drug loaded core–shell nanoparticles were separated from free DOX solution with centrifugation. The concentration of the remaining DOX solution was determined using a fluorescence spectrophotometer at λ_{ex}=475 nm and λ_{em}=592 nm, respectively. To confirm the amount of drug stored by the nanoparticles, a standard plot was prepared under identical conditions.

Cellular Experiments: The UCL emission of UCNPs was performed by a modified Laika laser-scanning microscope. And

Nanoscale Accepted Manuscript

This journal is © The Royal Society of Chemistry [year]

the cell nuclei were stained by 4,6-diamidino-2-phenylindole (DAPI). The *in vitro* cytotoxicity was measured using a standard methyl thiazolyl tetrazolium (MTT, Sigma Aldrich) assay. KB cells were seeded into 96-well cell culture plates at 1×10^4 per well incubated overnight at 3 °C in a humidified incubator, and then incubated with CCUCNPs@PM or DOX loaded CCUCNPs@PM at a concentration of 200 μg mL^{-1} for 2 h. After removal of nanoparticles, cells were transferred into fresh media and irradiated by the 980 nm laser for certain times (0.5 W cm^{-2}). The cells were then incubated at 37 °C for additional 24 h before the MTT assay.

In vivo experiments: KB cells (1×10^6 cells/site) were implanted subcutaneously into the leg of male athymic nude mice (4 weeks old). Each tumor was intratumorally injected with ca.50 μL saline, CCUCNPs@PM, or DOX loaded CCUCNPs@PM (10 mg mL^{-1} UCNPs). Laser irradiation was launched one day after the injection using an optical fiber-coupled 980 nm diode laser (Hi-Tech Optoelectronics Co., Ltd. Beijing, China), 0.5 W cm^{-2} for 30 min with a 1 min interval after each minute of irradiation. The tumor sizes were measured by a caliper every 2 days and calculated as the volume V = (tumor length) × (tumor width) $^2/2$. Relative tumor volumes were calculated as V / V_0, where V_0 was the tumor volume when the treatment was initiated.

In vivo UCL Imaging: The UCL *in vivo* image was performed by a modified Maestro in *vivo* imaging system using a 980 nm optical fiber coupled laser as the excitation source. The laser power density was ca. 0.2W cm^{-2} during imaging. An 850 nm short-pass emission filter was used to prevent the interference of excitation light to the CCD camera.

Results and Discussion

Characterizations of the CCUCNPs@PM

Preparation of UCNPs@mSiO2@C18@Ce-6 (CCUCNPs)

As the most efficient NIR-to-visible (green or blue) upconversion materials, Yb/Er (or Yb/Tm) co-doped NaYF4 nanocrystals are being increasingly used for bioimaging and cancer therapy.[26,27] To reduce the strong blue emission (around 475 nm) as well as an intense NIR (around 800 nm) emission exhibited by the currently used NaYF4-based UCNPs, here we prepared single-band upconversion emitting UCNPs with intense red light (650–670 nm) emission by manganese (Mn^{2+}) doping with a modified liquid-solid solution (LSS) solvothermal strategy. The doped Mn^{2+} ions into NaYF4:Yb/Er would change the transition possibilities of Er^{3+} and promote the transition of red emission. In this strategy, Y^{3+} ions were substituted by smaller Mn^{2+} ions in the host lattice, and smaller substitution ions tend to produce the cubic phase of the final products instead of hexagonal structures. On the other hand, hexagonal-to-cubic phase transformation would decrease the crystal field symmetry, and then the interplay of the doping rare earth ions in the different active sites would be changed, leading to reduce the inter quenching of Er^{3+} and then enhance UCL intensity. [28] The as-synthesized Mn^{2+}-doped UCNPs can be dispersed in nonpolar solvents and had an average diameter of about 20 nm according to the transmission electron microscopy (TEM) image (Fig. 1a). Energy dispersive spectrometry (EDS) analysis of individual nanocrystals evidenced the existence of manganese ions in our UCNPs (Fig. S1). From the X-ray diffraction pattern (XRD) of UCNP samples we could see a mixture of the cubic (JDPDS. 06-342) and hexagonal (JCPDS. 16-334) phases, and (JDPDS. 06-342) was the dominant phase (Figure 1d).

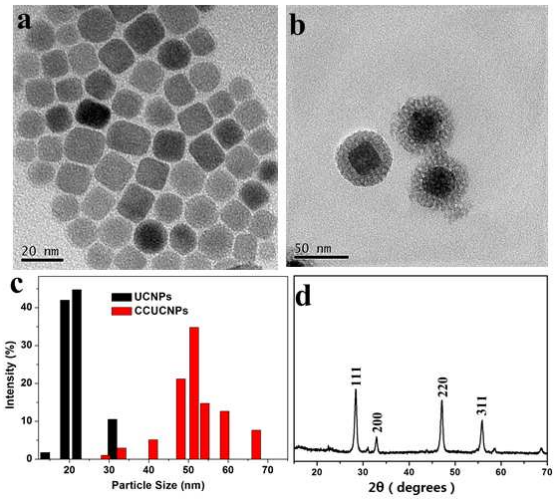

Fig. 1 TEM images of UCNPs (a), CCUCNPs (b), DLS data of UCNPs and CCUCNPs (c) and XRD of UCNPs (d).

To make the surface of Mn^{2+} -doped UCNPs nontoxic and easy to be modified, the particles were encapsulated by a mesoporous silica shell via the hydrolysis of tetraethylorthosilicate (TEOS) in a micro-emulsion system. In this strategy, hydrophobic nanoparticles were first transferred into aqueous media by utilizing cetyltrimethylammonium bromide (CTAB), and the CTAB also was used as the template of the mesoporous silica shell.[29] After removing the CTAB, long-chain hydrocarbonoctadecyltrimethoxysilane (C18) was introduced to graft onto the surface of silica for the self-assemble process combining with the amphiphilic copolymer, and then the grafting of Ce-6 was realized by reaction between the silica shell and Ce-6-3-aminopropyl) triethoxysilane. The obtained UCNPs@$mSiO_2$@C18-Ce6 (CCUCNPs) showed narrow distribution and had a particle size of about 50 nm according to the typical TEM image (Fig. 1b), in which one UCNPs core is encapsulated into one $mSiO_2$ shell, the results were also agree with the analyzes of Dynamic light scattering (DLS) (Fig. 1c). As shown in the spectrum of UCNPs@$mSiO_2$, a new strong bond of Si–OH (950 cm^{-1}) revealed the successful silica coating (Fig. S2). From the TEM images, we also confirmed that the surface of the silica shell was not destroyed after the grafting of C18 and Ce-6, and maintain good morphological features. To confirm the pore of silica shell was not blocked by these small organic molecules, N_2 adsorption–desorption isotherms and the correspondingpore size distributions was shown in Fig. S3, and the unblocked pore was important for the drug loading and release in further applications.[30]

As the generator of $^1O_2$, Ce-6 play a decisive role in our designed system. The grafting of Ce-6 would change the color of the particles, so the photograph of the CCUCNPs solution (inserted in Fig. 2a) could confirm the successful Ce-6 grafting. The strong absorbance peak at 660 nm in the UV-Vis spectra of Ce-6 (Fig. 2a) also demonstrated the grafting of Ce-6 in the CCUCNPs and the content of Ce-6 onto CCUCNPs was determined as 6.9% (w/w) by the UV quantitative analysis.[31]

Nanoscale Accepted Manuscript

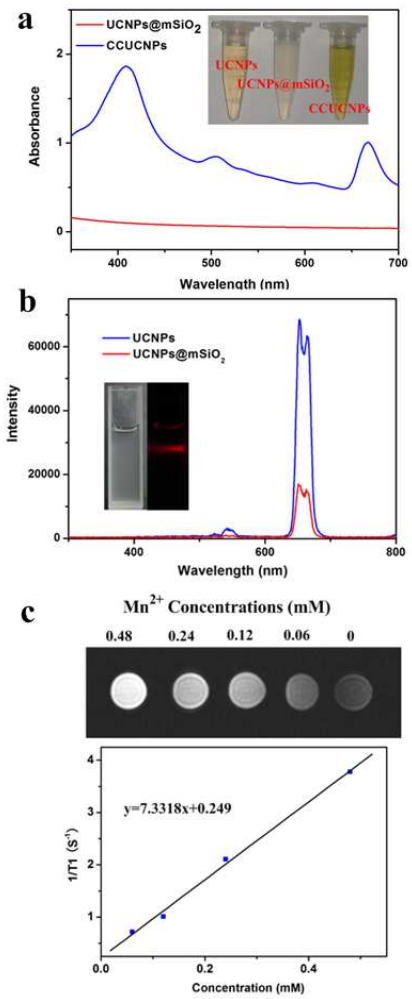

Fig. 2 Characterization of CCUCNPs. (a) UV-Vis of UCNPs@$mSiO_2$ and CCUCNPs; inset: photo of UCNPs, UCNPs@$mSiO_2$ and CCUCNPs solution. (b) A UCL emission spectrum of UCNPs and UCNPs@$mSiO_2$ under 980 nm laser excitation; insert: photo of a UCNPs@$mSiO_2$ solution under ambient light and under 980 nm laser excitation. (c) T_1-weighted MR images of UCNPs@$mSiO_2$ solutions at different concentrations and T_1 relaxation rates (r_1) of UCNPs@$mSiO_2$ solutions at different Mn^{2+} concentrations.

Before studying the singlet oxygen generation of our CCUCNPs, we should determine that upconversion luminescence (UCL) emission of UCNPs would not destroyed by the mesoporous silica shell. The UCL emission spectra of UCNPs and UCNPs@$mSiO_2$ was shown in Fig. 2b. Though a little decline was observed at 660 nm, it still provided a strong red light emission which was decisive for degradation of Ce-6 and further bioimaging. This result was in good agreement with the photo of a UCNPs@$mSiO_2$ solution under ambient light and under 980 nm laser excitation (insert Fig. 2b). It has been proved that manganese ions (Mn^{2+}) could be used as a T_1 contrast agent in MR imaging.[32,33] Our prepared CCUCNPs showed an obvious concentration-dependent brightening effect in the T_1-weighted phantom images of the nanocomposites at different concentrations, showing a transverse relaxivity(r_1) of 7.33 S^{-1} mM^{-1} on the basis of the Mn concentration, suggesting our nanoparticles a potential MR imaging agent (Fig. 2c).

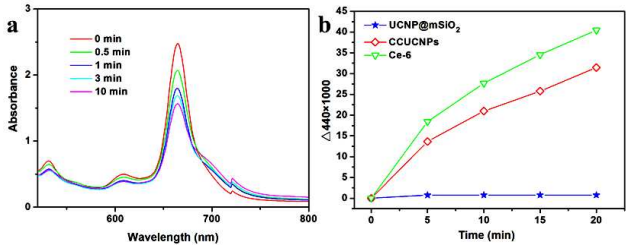

Fig. 3 Characterization of singlet oxygen generation. (a) UV-Vis spectra of CCUCNPs under different irradiation time. (b) Singlet oxygen generation by CCUCNPs under 980 nm laser irradiation.

Upon 980 nm irradiation, CCUCNPs with strong red light emission would activate Ce-6 to produce $^1O_2$,[34] an observed decline of UV-Vis absorbance at 660 nm with different irradiation time demonstrate the activation of Ce-6 (Fig. 3a). The bleaching of N,N-dimethyl-4-nitrosoaniline (RNO) was used to study the $^1O_2$ generation of our CCUCNPs complexes, the absorbance at 440 nm of RNO would be diminished in the presence of $^1O_2$. With different laser irradiation time, the $^1O_2$ generation was shown in Fig. 3b. Compared to same amount of pure Ce-6 under 660 nm light irradiation, CCUCNPs still proved to be a good $^1O_2$ generator when exposed in 980 nm laser.

Synthesis of amphiphilic copolymer (PM)

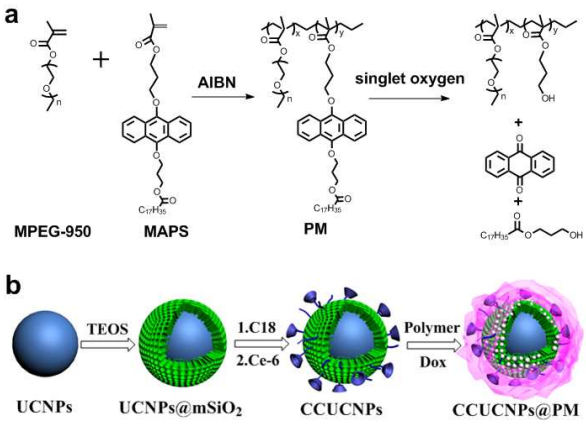

Scheme 2 Schematic illustration of a) the synthesis of PM and the degradation under singlet oxygen; b) the preparation of CCUCNPs@PM.

In earlier works, an amphiphilic copolymer with 9,10-dialkoxyanthracene (DN) groups was bound with Eosin by π-π stacking.[35] The polymer became degradable when exposed into visible light because the 9,10-dialkoxyanthracene (DN) would be changed into 9,10-anthraquinone (AQ) under appearance of $^1O_2$ produced by Eosin. In this study, DN contained hydrophobic monomer 3-((10-(3-(methacryloyloxy)propoxy) anthracen-9-yl)oxy)propyl stearate (MAPS) was synthesized as previous reported, and then copolymerized with Poly(ethylene glycol) methyl ether methacrylate-950 *via* typical radical polymerization to get the amphiphilic polymer (PM), as shown in Scheme 2.

The ^1H NMR spectra of the PM in different cases were shown in Fig. S4 where the signal of DN species was clearly shown. Then the previous prepared CCUCNPs was dispersed into the solution of the PM, When we applied a 980 nm laser (0.4 W cm^{-2}) to this solution for 20 min, two new aromatic signals appeared in the ^{1}HNMR spectrum and were proved to be from anthraquinone.

Nanoscale Accepted Manuscript

This journal is © The Royal Society of Chemistry [year]

To further confirm the photocleavage of the PM, GPC measurement was done post 20 min laser irradiation. The decrease of M_n with the stirred time is shown in Fig. S5. Without laser irradiation, the M_n of the PM showed almost no change, but after the 980 nm laser irradiation, a sharp decrease in M_n indicated the $^1O_2$-mediated reaction had occurred and the polymer was cleaved. This result suggested the conversion of hydrophobic segments of PM to hydrophilic ones, with the appearance of CCUCNPs when exposed to 980 nm laser.

Preparation of CCUCNPs@PM

CCUCNPs@PM was prepared via self-assembly process (Scheme 2). PM was first dissolved in tetrahydrofuran, and then CCUCNPs was dispersed in this solution followed by the addition of distilled water. After evaporation of the THF at room temperature, the prepared amphiphilic PM would form micelles in water and hydrophobic CCUCNPs would be encapsulated to form core-shell nanocomposites, and long alkyl chains of hydrophobic groups of polymer would strongly associate with the hydrophobic C18 alkyl chains on the CCUCNPs surface through hydrophobic *van der Waals* interactions.[36,37] The detailed morphological features of the prepared nanoparticles were examined by TEM. As shown in Fig. S6, the surface of the nanoparticles became smooth and the profile of the CCUCNPs@PM became blurred. A boundary line between the polymer film and the silica shell could be clearly observed in the enlarged TEM images of the nanocomposites (insert of Fig. S6), which further confirmed the encapsulation of the polymer film. Furthermore, the prepared CCUCNPs@PM still retained a good monodispersity with an average diameter of about 65 nm, which was in accordance with the findings from the dynamic light scattering (DLS) measurements (Fig. S7).

Drug Loading and Drug/$^1O_2$ Release Assay in Solution

DOX was used here as a model anti-cancer drug, to examine the drug loading and release behaviour of the CCUCNPs@PM. DOX was extracted from doxorubicin hydrochloride (DOX·HCl) according to the procedure reported previously.[38] The DOX solution (5 mg mL^{-1}) was added in the self-assembly procedure of CCUCNPs@PM. And then DOX-loaded CCUCNPs@PM was obtained after centrifugation and washed with water for several times. To evaluate the drug loading capacity here, fluorescence spectrophotometer was used and DOX loading in the formulation was determined as 105±8 mg of drug per mg of nanocomposite. The nanocomposites encapsulated DOX efficiently (a loading efficiency of about 79%), which was sufficient to be injected to kill cancer cells.

The *in vitro* release profiles of DOX and $^1O_2$ from the DOX-loaded CCUCNPs@PM in PBS buffer in response to 980 nm laser was showed in Fig. 4a, each irradiation time lasted for 5 min at 5 min intervals. Without any stimuli, only less than 5% of DOX was released after 8 h. When we exerted laser irradiation, a burst release (>70% in 8 h) was observed from the uncovered pore of silica shell due to the degradation of PM. Under the same irradiation time, the singlet oxygen generation was studied to confirm the excess release of $^1O_2$. It can be proved that there were still excess $^1O_2$ can be determined in the solution after the degradation of polymer and the $^1O_2$ release was photo controlled, which is important for the further dual cancer therapy.

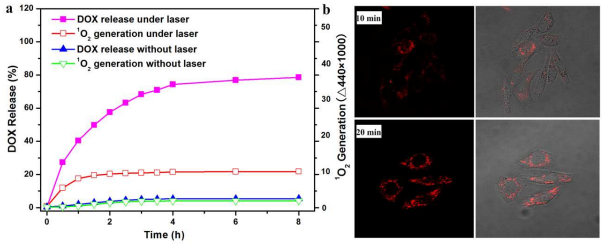

Fig. 4 a) Release profiles of DOX and $^1O_2$ from CCUCNPs@PM nanocarriers in PBS buffer with or without laser irradiation at 980 nm at power density of 1.22 W, b) CLSM of intracellular location of DOX after laser irradiation.

To further study the cellular uptake of DOX-loaded CCUCNPs@PM nanospheres and the cellular drug release, confocal laser scanning microscope (CLSM) was used to determine the location of DOX after the laser irradiation. As shown in Fig. 4b, after incubation of KB cells with the samples for 1 h and laser irradiation for 10 min, intracellular red fluorescence was observed, localized in the perinuclear area of the cytoplasm, demonstrating that the DOX-loaded hybrid nanocarrier have been taken up by KB cells and DOX release from DOX loaded CCUCNPs@PM. After 980 nm irradiation for another 10 min, a significant enhancement of fluorescence signal can be observed, further confirming the release of the pre-loaded DOX from CCUCNPs@PM.

Evaluations of the NIR-Triggered therapeutic application Using Cell and Animal Models

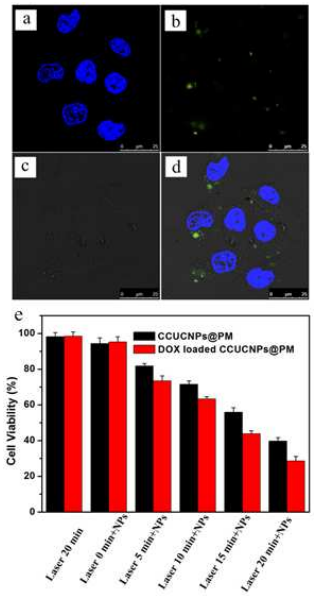

Fig. 5 Confocal laser scanning microscopy imaging of KB cells after being incubated with CCUCNPs@PM for 2 h (a-d). Green: the UCL emission from UCNPs, Blue: DAPI (nuclear staining),and the overlay at dark-field image and bright field image. e) Cell viability data of KB cells after various treatments indicated with and without the 980 nm laser irradiation as evaluated by the standard MTT Assay. Error bars are based on four parallel samples.

Mn^{2+}-doped UCNPs have been proven to be a promising tool for biomedical imaging and cancer therapy. In our present study, we also used time course UCL microscopy to investigate the interaction between KB cells and the CCUCNPs@PM by

Nanoscale Accepted Manuscript

utilizing a modified inverted CLSM equipped with infrared laser excitation at 980 nm. After incubation with CCUCNPs@PM (200 ug mL^{-1}) for 2 h, the surface-attached nanoparticles were removed, the cells were washed with abundant PBS and then transferred into fresh media. Then the cells were investigated by CLSM with an external 980 nm source (Fig. 5a-d). From the CLSM pictures, obvious UCL signal of bright green luminescence coming from CCUCNPs@PM can be observed in the dark, overlays of bright field and DAPI stained nuclear CLSM images further demonstrate that the luminescence was evident in the intracellular region. This observation demonstrated the ability of CCUCNPs@PM for high-contrast *in vitro* cell imaging.

The *in vitro* cytotoxicity of CCUCNPs@PM and DOX-loaded CCUCNPs@PM under 980 nm light irradiation was evaluated by the MTT assay. We incubated KB cells in the culture medium with CCUCNPs@PM and DOX-loaded CCUCNPs@PM under NIR-light excitation, comparing with DOX-loaded CCUCNPs@PM without NIR-light excitation as the controls. After 3 h of incubation, the excess nanoparticles were removed and the cells were further incubated for 24 h in the dark. From Fig. 5e, no significant decrease in cell viability could be observed with treatment of CCUCNPs@PM and DOX-loaded CCUCNPs@PM without laser irradiation, indicating that our prepared nanocomposites with a PEG outsurface was much biocompatible, also demonstrating negligible delivery of DOX into the KB cells because of the absence of an impelling effect of the amphiphilic polymer. In contrast, CCUCNPs@PM and DOX-loaded CCUCNPs@PM upon 980 nm laser irradiation showed a significantly enhanced cytotoxicity to the cancer cells, further confirming the photocontrolled release and significant accumulation of DOX inside the cells. On the other hand, it worth noted that CCUCNPs@PM without DOX loading provide a good therapeutic result for the $^1O_2$ release upon NIR-light irradiation, and a significant enhancement cytotoxicity result in DOX-loaded CCUCNPs@PM upon 980 nm laser because of both DOX and $^1O_2$ release from the nanocomposites after the degradation of PM upon laser irradiation. The toxicity of nanocomposite after degradation also was investigated. CCUCNPs@PM was first dispersed in PBS and then nanocomposite was degraded under laser irradiation. After centrifugation, the precipitate was redispersed and was used to evaluate the toxicity of nanocomposite after degradation. The results was shown in Fig. S8. This finding is in line with previous drug release experiment, strongly demonstrating that our designed nanocompsites show fast responsivity to laser irradiation and have a better therapeutic result than single PDT or PDD. To further study the performence of DOX loaded CCUCNPs@PM for in *vivo* cancer therapy, athymic nude mice bearing KB cells were randomized into 3 treatment groups: salin with laser treated (Group 1), CCUCNPs@PM with laser treated (Group 2), DOX-loaded CCUCNPs@PM with laser treated (Group 3). Each mice was intratumorally (i.t.) injected with ca.50 μL saline, CCUCNPs@PM, or DOX loaded CCUCNPs@PM (10 mg mL^{-1} UCNPs), followed by exposure of 980-nm irradiation (0.5 W cm^{-2}) for 30 min, with 1 min intervals every 1 min. The tumor size was examined every 2 day and the tumor growth rate were monitored after the treatment. As can be seen in Fig. 6a, treatment with saline and laser could not delay the growth of tumor, compared to the control group, the tumor growth was retarded in both CCUCNPs@PM and DOX-loaded CCUCNPs@PM treated groups with laser irradiation. Meanwhile, DOX-loaded CCUCNPs@PM treated group showed a much slower tumor growth rate for the $^1O_2$ and DOX release. Mice were then sacrificed at 23rd day and the the tumor tissues were collected, the picture of the tumor futher suggests the tumor shrinkage caused by CCUCNPs@PM and DOX-loaded CCUCNPs@PM (Fig. S9).

The histology studies were lunched after the mice were sacrificed, major organs were collected and then undergo H&E staining, results were shown in Fig. 6b which confirmed that the treatment with both CCUCNPs@PM and DOX-loaded CCUCNPs@PM caused little impact to the liver, as well as to other major organs.

For the Mn^{2+}-doped nanoparticles coulde convert NIR light to red light, obviously red UCL emission signals of UCNPs could be observed from tumors on mice even at 3 days after the i.t. injection of CCUCNPs@PM, revealing that our CCUCNPs@PM had a good performence in *vivo* imaging and could retain at the tumor site for a longer time (Fig. 6c). Hence, the application of CCUCNPs@PM can prolong the time interval between drug administrations, leading to reduced patient suffering.

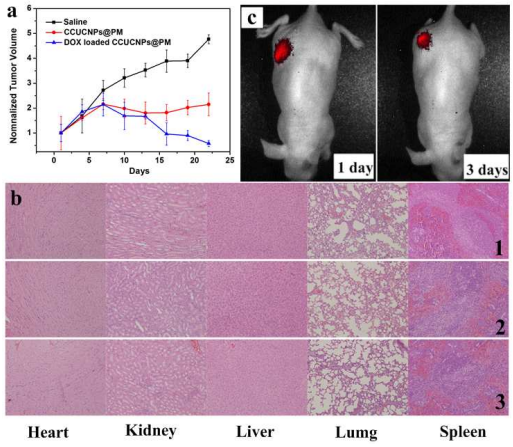

Fig. 6 a) Comparison of the tumor inhibition effect of saline, CCUCNPs@PM and DOX-loaded CCUCNPs@PM. b) H&E staining with normal tissues: 1) control, 2) CCUCNPs@PM and 3)DOX-loaded CCUCNPs@PM. c) UCL images of CCUCNPs@PM .

Conclusions

In summary, a multifunctional nanocomposite was prepared by coating a NIR light-responsive amphiphilic copolymer onto the C18- and Ce-6-modified UCNPs for synchronous NIR light-triggered chemotherapy and photodynamic therapy. Upon NIR light irradiation, both CCUCNPs@PM and DOX-loaded CCUCNPs@PM showed good therapeutic effects *in vitro* and *in vivo*. And compared to PDT alone in CCUCNPs@PM treatment, anticancer drug release from DOX-loaded CCUCNPs@PM enhances the cancer therapeutic efficiency. The UCNPs encapsulated endow this theranostic composite cell imaging and could be further used to trigger the drug release and photodynamic therapy. We expect that our strategy of combinating the NIR light-triggered controlled drug release and PDT methods in one nanodevice could pave the way for the

Nanoscale Accepted Manuscript

This journal is © The Royal Society of Chemistry [year]

development of other multifunctional photo-responsive drug delivery systems in the future.

Acknowledgements

We gratefully acknowledge the financial support provided by National Natural Science Foundation of China (21336005, 21301125), Natural Science Foundation of Jiangsu Province (BK2012625), Natural Science Foundation of the Jiangsu Higher Education Institutions of China (13KJB430022), Innovation and Entrepreneurship Training Program for Students of Soochow University, 2013 (2013xj024) and Joint Research Projects of SUN-WIN Joint Research Institute for Nanotechnology.

Notes and references

[a] *College of Chemistry, Chemical Engineering and Materials Science, Collaborative Innovation Center of Suzhou Nano Science and Technology, Soochow University, Suzhou, 215123, China*
[b] *Functional Nano & Soft Materials Laboratory (FUNSOM) and Jiangsu Key Laboratory for Carbon-Based Functional Materials & Devices, Soochow University, Suzhou, Jiangsu 215123, China*

1 R. Liu, X. Zhao, T. Wu, P. Feng, *J. Am. Chem. Soc.,* 2008, **130**, 14418.
2 C. Park, K. Oh, S. C. Lee, C. Kim, *Angew. Chem. Int. Ed.,* 2007, **46**,1455.
3 D.Y. Chen, Z.T. Luo , N.J. Li, J. Y. Lee, J.P. Xie and J.M. Lu, *Adv. Funct. Mater.,* 2013, **23**, 4324.
4 C. Coll, L. Mondragon, R. Martinez-Manez, F. Sancenon, M. Dolores Marcos, J. Soto, P. Amoros, E. Perez-Paya, *Angew. Chem. Int., Ed.* 2011, **50**, 2138.
5 N. Fomina, J. Sankaranarayanan, A. Almutairi, *Adv. Drug Delivery Rev.,* 2012, **64**, 1005.
6 D. Wang, G. Ye, Y. Zhu and X. Wang, *Macromolecules*, 2009, **42**, 2651.
7 J. del Barrio, L. Oriol, C. Sanchez, J. L. Serrano, A. Di Cicco, P. Keller and M. H. Li, *J. Am. Chem. Soc.,* 2010, **132**, 3762.
8 Q. N. Lin, C. Y. Bao, S. Y. Cheng, Y. L. Yang, W. Ji, L.Y. Zhu, *J.Am. Chem. Soc.,* 2012, **134**, 5052.
9 B. Yan, J. C. Boyer, D. Habault, N. R. Branda and Y. Zhao, *J. Am. Chem. Soc.,* 2012, **134**, 16558.
10 Q. N. Lin , C. Y. Bao, Y. L. Yang, Q. N. Liang, D. S. Zhang, S. Y. Cheng, L. Y. Zhu, *Adv. Mater.,* 2013, **25**, 1981.
11 S. Yang, N. J. Li, D. Y. Chen, X. X. Qi, Y.J. Xu, Y. Xu, Q. F. Xu, H. Li and J. M. Lu, *J. Mater. Chem. B,* 2013, **1**, 4628.
12 G. S. Kumar and D. C. Neckers, *Chem. Rev.,* 1989, **89**, 1915.
13 Esther Amstad, Shin-Hyun Kim, and David A. Weitz, *Angew. Chem. Int. Ed.,* 2012, **51**, 1.
14 N. Li, Z.Z. Yu, W. Pan, Y. Y. Han, T.T. Zhang and B. Tang, *Adv. Funct. Mater.,* 2013, **23**, 2255.
15 J. N. Liu, W. B. Bu, L.M. Pan and J. L. Shi, *Angew. Chem. Int. Ed.,* 2013, **52**, 1.
16 Y. M. Yang, Q. Shao, R. R. Deng, C. Wang, X. Teng, K. Cheng, Z. Cheng, L. Huang, Z. Liu, X. G. Liu and B. G. Xing, *Angew. Chem. Int. Ed.,* 2012, **51**, 3125.
17 L. Z. Zhao, J. J. Peng, Q. Huang, C. Y. Li, M. Chen, Y. Sun, Q. N. Lin, L. Y. Zhu and F. Y. Li, *Adv. Funct. Mater.,* 2014, **24**,363.
18 Gross. S, Gilead. A, Scherz. A, Neeman. M, Salomon. Y, *Nat. Med.,* 2003, **9**, 1327.
19 Z. P. Zhen, W. Tang, C. L. Guo, H. M. Chen, X. Lin, G. Liu, B. W. Fei, X. Y. Chen, B. Q. Xu and J. Xie, *ACS Nano,* 2013, **7**, 6988.
20 Agostinis. P, Berg. K, Cengel. K. A, Foster. T. H, Girotti. A. W, Gollnick. S. O, Hahn. S. M, Hamblin. M. R, Juzeniene. A and Kessel. D, *Cancer J. Clin*., 2011, **61**, 250.
21 S. S. Cui, D. Y. Yin, Y. Q. Chen, Y. F.Di, H. Y. Chen, Y. X. Ma, S. Achilefu, and Y. Q. Gu, *ACS Nano,* 2013, **7**, 678.
22 H. C. Guo, H. S. Qian, N. M. Idris, Y. Zhang, *Nanomed.: Nanotechnol. Biol. Med.,* 2010, **6**, 486.
23 P. Zhang, W. Steelant, M. Kumar, M. Scholfield, *J. Am. Chem. Soc.,* 2007, **129**, 4526.
24 N. M. Idris, M. K. Gnanasammandhan, J. Zhang, P. C. Ho, R. Mahendran, Y. Zhang, *Nat. Med.,* 2012, **18**, 1580.
25 H. S. Qian , H. C. Guo, P. C. Ho, R. Mahendran, Y. Zhang, *Small,* 2009, **5**, 2285.
26 M. Haase, H. Schafer, *Angew. Chem. Int. Ed.,* 2011, **50**, 5808.
27 J. Zhou, Y. Sun, X. Du, L. Xiong, H. Hu, F. Li, *Biomaterials,* 2010, **31**, 3287.
28 G. Tian, Z. J. Gu, L. J. Zhou, W. Y. Yin, X. X. Liu, L. Yan, S. Jin, W. L. Ren, G. M. Xing, S. J. Li, and Y. L. Zhao, *Adv. Mater.,* 2012, **24**, 1226.
29 G. S. Song, Q. Wang, Y. Wang , G. Lv, C. Li, R. J. Zou, Z. G. Chen, Z, Y. Qin, K. K. Huo, R. G. Hu and J. Q. Hu, *Adv. Funct. Mater.,* **2013**, **23**, 4281.
30 X. Mei, S. Yang, D. Y. Chen, N. J. Li, H. Li, Q. F. Xu, J. F. Ge and J. M. Lu, *Chem. Commun.,* 2012, **48**, 10010.
31 C. Wang, L. Cheng, Y. M. Liu, X. J. Wang, X. X. Ma, Z. Y. Deng, Y. G. Li, and Z. Liu, *Adv. Funct. Mater.,* 2013, **23**, 3077.
32 S J. Jackson, R. Hussey, M. A. Jansen, G. D. Merrifield, I. Marshall, A. MacLullich, J. L. W. Yau, T. Bast, *Behav. Brain Res.,* 2011, **216**, 293.
33 A. Bertin, J. Steibel, A. I. Michou-Gallani, J. L. Gallani, D. Felder-Flesch, *Bioconjugate Chem.,* 2009, **20**, 760.
34 C. Wang, H. Tao, L. Cheng, Z. Liu, *Biomaterials,* 2011, **32**, 6145.
35 Q. Yan, J. Hu, R. Zhou, Y. Ju, Y. W. Yin and J. Y. Yuan, *Chem. Commun.,* 2012, **48**, 1913.
36 E. Aznar, L. Mondragon, J. V. Ros-Lis, F. Sancenon, M. D. Marcos, R. Martinez-Manez, J. Soto, E. Perez-Paya and P. Amoros, *Angew. Chem.Int. Ed.,* 2011, **50**, 11172.
37 D. Y. Chen, N. J. Li, H. W. Gu, X. W. Xia, Q. F. Xu, J. F. Ge, J. M. Lu and Y. G. Li, *Chem. Commun.,* 2010, **46**, 6708.
38 Y. Gao, Y. Chen, X. F. Ji, X. Y. He, Q. Yin, Z. W. Zhang, J. L. Shi and Y. P. Li, *ACS Nano,* 2011, **5**, 9788.

Nanoscale Accepted Manuscript